in GenBank and from the Genome Sequencing Centre Jena (http://genome.imb-jena.de/dictyostelium/). Primers were designed to amplify the repeat sequence (information is available from the authors on request), which is often variable in length.

To determine if clones mix, we performed 15 pairwise mixing experiments. For each, we grew up fruiting bodies for the two clones separately, picked 5 sori from each, and mixed all 10 with *Klebsiella aerogenes* as a food source in 0.2 ml of sterile distilled water, where they dispersed as hundreds of thousands of independent amoebae. We spread this homogeneous mixture of two clones out on an SM/5 plate. After several days growth at 22 °C, the starving amoebae aggregated and formed migrating slugs, and 24 were chosen for genotyping at a microsatellite locus chosen because the two parent clones possessed different alleles. Mixing was confirmed if a slug showed both parental alleles. We mixed all the clone pairs listed in Fig. 2 except NC94.1-NC94.2 (which did not grow in this trial), plus four others: NC41.2-NC67.2; NC54.1-NC54.2; NC42.1-NC43.1; and NC66.2-NC 85.1. We use the original nomenclature[16].

To assess the frequency of cheating in mixtures, we made 12 pairwise mixtures (listed in Fig. 2) as in the first experiment. For each mixture, we selected 7 migrating slugs. The front 10% of the slug was excised as a sample of the prestalk region. The prespore region of each slug was sampled twice, using the posterior 10% of the slug and an equivalent portion from the middle of the prespore region. We extracted DNA separately from all three portions and amplified a microsatellite locus that differed for the two parent clones, incorporating ^{35}S-labelled dATP in the PCR reaction. We ran the product DNA out on a 6% polyacrylamide gel. We then quantified the relative amounts of the two parental alleles using a phosphorimager that measures the radiation given off by any region of the gel. To remove background, we subtracted the average radiation reading of two other areas, located above and below the bands, and identical in size to the band. Exposures were kept low to avoid saturation effects. We compared the prestalk with the average of the two prespore samples. A replicate set of the same 12 mixtures was conducted, using only the posterior 10% of the slug for the prespore region, and 11 of the 12 showed differences in the same directions as in Fig. 2.

Marker loci were chosen such that the two alleles did not have overlapping stutter bands, but were within a few repeats of each other to avoid differential amplification. However, even if the one of the two alleles amplified better, it would do so consistently in prestalk and prespore samples, so that a test for a difference between these two samples remains valid. We confirmed that the method works by amplifying a second locus for five of our mixtures. For each, the correlation across slugs of two locus-specific estimates of %prestalk minus %prespore was highly significant ($P < 0.005$) with the correlation averaging 0.8. If the results we reported were due to differential amplification or some other artefact, we would expect no correlation, or negative correlations as often as positive.

Received 15 September; accepted 18 October 2000.

1. Maeda, Y., Inouye, K. & Takeuchi, I. (eds) *Dictyostelium—A Model System for Cell and Developmental Biology* (Universal Academy, Tokyo, 1997).
2. Gross, J. D. Developmental decisions in *Dictyostelium discoideum*. *Microbiol. Rev.* **58,** 330–351 (1994).
3. Bonner, J. T. *The Cellular Slime Molds* (Princeton Univ. Press, Princeton, 1967).
4. Raper, K. B. *The Dictyostelids* (Princeton Univ. Press, Princeton, 1984).
5. Raper, K. B. Pseudoplasmodium formation and organization in *Dictyostelium discoideum*. *Journal of the Elisha Mitchell Scientific Society* **56,** 241–282 (1940).
6. Williams, G. C. *Adaptation and Natural Selection: A Critique of Some Current Evolutionary Thought* (Princeton Univ. Press, Princeton, 1966).
7. Gadagkar, R. & Bonner, J. T. Social insects and social amoebae. *J. Biosci.* **19,** 219–245 (1994).
8. Armstrong, D. P. Why don't cellular slime molds cheat. *J. Theor. Biol.* **109,** 271–283 (1984).
9. Buss, L. W. Somatic cell parasitism and the evolution of somatic tissue compatibility. *Proc. Natl Acad. Sci. USA* **79,** 5337–5341 (1982).
10. Hilson, J. A., Kolmes, S. A. & Nellis, L. F. Fruiting body architecture, spore capsule contents, selfishness, and heterocytosis in the cellular slime mold, *Dictyostelium discoideum*. *Ethol. Ecol. Evol.* **6,** 529–535 (1994).
11. Wilson, D. S. & Sober, E. Reviving the superorganism. *J. Theor. Biol.* **136,** 337–356 (1989).
12. Kessin, R. H. in *Dictyostelium—A Model System for Cell and Developmental Biology* (eds Maeda, Y., Inouye, K. & Takeuchi, I.) 3–13 (Universal Academy, Tokyo, 1997).
13. Atzmony, D., Zahavi, A. & Nanjundiah, V. Altruistic behaviour in *Dictyostelium discoideum* explained on the basis of individual selection. *Curr. Sci.* **72,** 142–145 (1997).
14. Huss, M. J. Dispersal of cellular slime moulds by two soil invertebrates. *Mycologia* **81,** 677–682 (1989).
15. Hamilton, W. D. The genetical evolution of social behaviour. I, II. *J. Theor. Biol.* **7,** 1–52 (1964).
16. Francis, D. & Eisenberg, R. Genetic structure of a natural population of *Dictyostelium discoideum*, a cellular slime mold. *Mol. Ecol.* **2,** 385–391 (1993).
17. Ketcham, R. B. & Eisenberg, R. M. Clonal diversity in populations of *Polysphondylium pallidum*, a cellular slime mold. *Ecology* **70,** 1425–1433 (1989).
18. Grosberg, R. K. The evolution of allorecognition specificity in clonal invertebrates. *Q. Rev. Biol.* **63,** 377–412 (1988).
19. Filosa, M. F. Heterocytosis in cellular slime molds. *Am. Nat.* **96,** 79–91 (1962).
20. Houle, J., Balthazar, J. & West, C. M. A glycosylation mutation affects cell fate in chimeras of *Dictyostelium discoideum*. *Proc. Natl. Acad. Sci. USA* **86,** 3679–3683 (1989).
21. Ennis, H. L., Dao, D. N., Pukatzki, S. U. & Kessin, R. H. *Dictyostelium* amoebae lacking an F-box protein form spores rather than stalk in chimeras with wild type. *Proc. Natl Acad. Sci. USA* **97,** 3292–3297 (2000).
22. Velicer, G. J., Kroos, L. & Lenski, R. E. Developmental cheating in the social bacterium *Myxococcus xanthus*. *Nature* **404,** 598–601 (2000).
23. Stoner, D. S., Rinkevich, B. & Weissman, I. L. Heritable germ and somatic cell lineage competitions in chimeric colonial protochordates. *Proc. Natl Acad. Sci. USA* **96,** 9148–9153 (1999).
24. Grosberg, R. K. & Quinn, J. F. The genetic control and consequences of kin recognition by the larvae of a colonial marine invertebrate. *Nature* **322,** 456–459 (1986).
25. Dawkins, R. & Krebs, J. R. in *Behavioural Ecology: An Evolutionary Approach* 2nd edn (eds Krebs, J. R. & Davies, N. B.) 282–309 (Blackwell, Oxford, 1978).
26. Elgar, M. A. & Nash, D. R. Sexual cannibalism in the garden spider *Araneus diadematus*. *Anim. Behav.* **36,** 1511–1517 (1988).
27. Queller, D. C. & Strassmann, J. E. Kin selection and social insects. *Bioscience* **48,** 165–175 (1998).
28. Loomis, W. F. *Four Billion Years; An Essay on the Evolution of Genes and Organisms* (Sinauer, Sunderland, Massachusetts, 1988).
29. Kay, R. R. & Williams, J. G. The *Dictyostelium* genome project—an invitation to species hopping. *Trends Genet.* **15,** 294–297 (1999).
30. Holm, S. A simple sequentially rejective multiple test procedure. *Scand. J. Statist.* **6,** 65–70 (1979).

Acknowledgements

We thank R. Gomer for advice and training; D. Welker for supplying the clones; J. Keay, W. Castle, S. Reddy and J. Damon for assistance with laboratory work; and D. Rozen, R. Kessin, G. Velicer and J. Bonner for comments on the manuscript. This work was supported in part by the US National Science Foundation.

Correspondence and requests for materials should be addressed to J.E.S. (e-mail: strassm@rice.edu).

Asymmetric leaves1 mediates leaf patterning and stem cell function in *Arabidopsis*

Mary E. Byrne*, Ross Barley†, Mark Curtis*‡, Juana Maria Arroyo*, Maitreya Dunham*‡, Andrew Hudson† & Robert A. Martienssen*

* *Cold Spring Harbor Laboratory, 1 Bungtown Road, Cold Spring Harbor, New York 11724, USA*

† *Institute of Cell and Molecular Biology, University of Edinburgh, Edinburgh EH9 3JR, UK*

Meristem function in plants requires both the maintenance of stem cells and the specification of founder cells from which lateral organs arise. Lateral organs are patterned along proximodistal, dorsoventral and mediolateral axes[1,2]. Here we show that the *Arabidopsis* mutant *asymmetric leaves1* (*as1*) disrupts this process. *AS1* encodes a myb domain protein, closely related to *PHANTASTICA* in *Antirrhinum* and *ROUGH SHEATH2* in maize, both of which negatively regulate knotted-class homeobox genes. *AS1* negatively regulates the homeobox genes *KNAT1* and *KNAT2* and is, in turn, negatively regulated by the meristematic homeobox gene *SHOOT MERISTEMLESS*. This genetic pathway defines a mechanism for differentiating between stem cells and organ founder cells within the shoot apical meristem and demonstrates that genes expressed in organ primordia interact with meristematic genes to regulate shoot morphogenesis.

The shoot apical meristem (SAM) comprises slowly dividing stem cells at the centre and daughter cells at the periphery, from which organ founder cells are recruited. Founder cells divide rapidly, initiating the outgrowth of organ primordia while polarity is established along the proximodistal, dorsoventral and mediolateral axes[1,2]. The mechanism by which stem cell and founder cell derivatives are distinguished is obscure, but is likely to involve a highly conserved class of homeobox genes related to *KNOTTED1* in maize (*KNOX* genes). *KNOX* genes are expressed in the SAM but are downregulated in founder cells at the time of leaf initiation[3]. They are implicated in maintaining division or preventing differentiation of cells in the SAM. Loss-of-function mutations in the *Arabidopsis KNOX* gene *SHOOT MERISTEMLESS* (*STM*) result in embryos that lack a SAM[4,5]. Recessive mutations in the *kn1* gene of maize are also defective in meristem maintenance[6]. In contrast, gain-of-function mutations that result in ectopic expression of *KNOX* genes in maize disrupt normal leaf development causing distal displacement

‡ Present address: Institute of Biological Sciences, University of Wales, Aberystwyth, UK (M.C.); Genetics Department, Stanford, California 94305, USA (M.D.).

of sheath and auricle tissue into the blade[7]. In dicotyledonous plants, such as *Arabidopsis* and tobacco, misexpression of homeobox transgenes results in lobed leaves, distally displaced stipules, and occasional ectopic meristems on the adaxial leaf surface[8,9].

PHANTASTICA (*PHAN*) in *Antirrhinum* is transcribed in organ founder cells and is required to prevent expression of an *STM*-like *KNOX* gene in lateral organs[10,11]. *phan* mutants show variable defects in leaf patterning, affecting both dorsoventral and proximodistal axes[12]. *PHAN* has a myb domain found in several transcription factors and its homologue in maize is *ROUGH SHEATH2* (*RS2*)[11,13]. Mutations in *RS2* result in phenotypes comparable to dominant mutations in *KNOX* genes, and show ectopic expression of homeodomain proteins in developing leaves revealing a conserved role for *RS2* in repressing *KNOX* gene expression[11,13,14].

asymmetric leaves1 (*as1*) is a classical mutation in *Arabidopsis* that disrupts development of cotyledons, leaves and floral organs (Fig. 1)[15]. The mutant leaf lamina is subdivided into prominent outgrowths or lobes. Early leaves have few lobes located proximally, whereas later leaves have more lobes extending distally toward the leaf tip (Fig. 1c). Adult rosette leaves of *magnifica*, the first isolated mutant allele of *as1* (ref. 16), have patches of callus-like growth on the leaf lamina, and occasionally have ectopic shoots on the adaxial surface of the petiole (Fig. 1d), similar to those observed in transgenic plants misexpressing the *KNOX* gene *KNAT1* (ref. 9). In wild-type leaves the abaxial epidermis over the midvein of the leaf petiole and blade is comprised of elongated cells (Fig. 1e). In *as1* there are multiple bundles of elongated cells extending from the petiole into the blade (Fig. 1f). The enhancer trap (see Methods) ET2689 marks these elongated cells (Fig. 1g) and is expressed over a much broader region in *as1* extending in multiple directions from the petiole (Fig. 1h). This pattern reflects a change in proximodistal and mediolateral patterning of the leaf.

Loss of *AS1* activity causes defects that are similar, in many respects, to those caused by misexpression of *KNOX* transgenes[1]. We used polymerase chain reaction after reverse transcription of RNA (RT–PCR) to examine expression of the *KNOX* genes *STM*, *KNAT1* and *KNAT2* in *as1* mutants. *STM* expression in the wild type is confined to SAM cells and is absent from leaves and leaf primordia[17]. No change in the pattern of expression was detected in *as1* (Fig. 2) even at the level of *in situ* hybridization (data not shown). *KNAT1* transcripts in wild-type plants were detected in whole-shoot and inflorescence tissue but not in leaves (Fig. 2), consistent with the reported expression pattern[18]. However, *KNAT1* was ectopically expressed in *as1* leaves (Fig. 2) and, as shown by *in situ* hybridization, was ectopically expressed in the cotyledons of *as1* embryos consistent with their altered morphology (Fig. 3l and m). *KNAT2* transcripts were present at high levels in wild-type shoot and inflorescence tissue as expected[19], but also at a low level in wild-type leaves (Fig. 2). In *as1* mutant leaves, expression of *KNAT2* was upregulated (Fig. 2).

We used positional cloning to identify the *AS1* gene. *as1* had previously been mapped to chromosome 2 (ref. 15). Phenotypic and molecular markers were used to map *as1* within a 1.0-centi-Morgans (cM) interval proximal to *det2*. The Arabidopsis Genome Initiative sequence in this region[20] revealed a likely candidate for

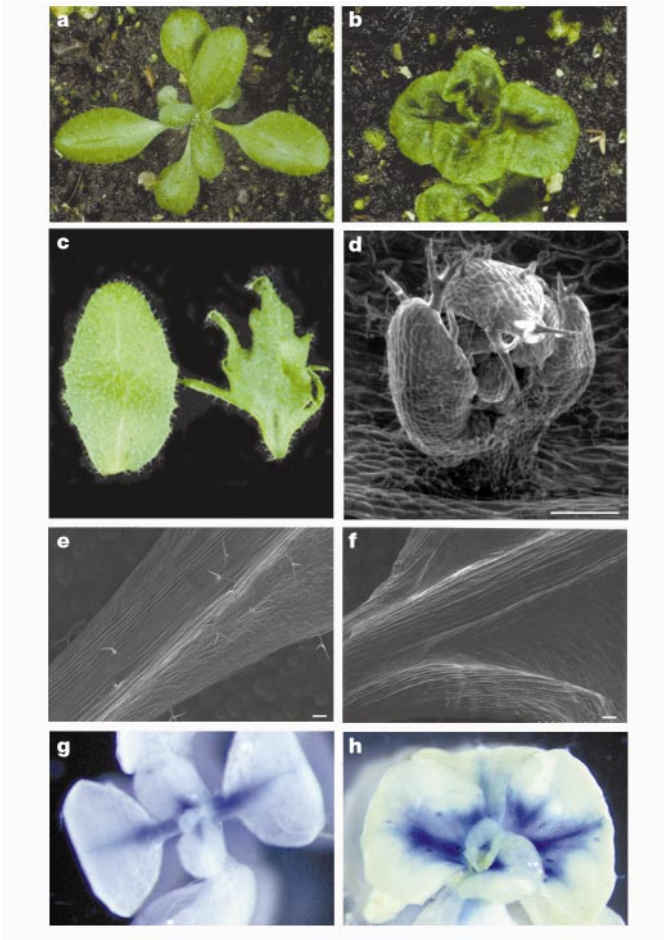

Figure 1 Comparison of *as1* mutant and wild-type *Arabidopsis*. **a**, Vegetative rosette of wild-type. Rosette leaves are elongate and spatulate in shape. **b**, Vegetative rosette of *as1*. Leaves are shorter than wild-type and have a rumpled appearance. **c**, Cauline leaf of the wild type (left), *as1* (right). The *as1* leaf has marginal lobes. **d**, Ectopic shoot in *magnifica*. **e**, Abaxial surface of wild-type leaf at the distal end of the petiole, showing elongated cells of the midvein. **f**, Abaxial surface of *as1* leaf. Elongated epidermal cells typical of the midvein occur in multiple files. **g**, ET2689 in the wild type marks cells of the midvein. **h**, In *as1* ET2689 shows much broadened GUS expression. Scale bars, 200 μm.

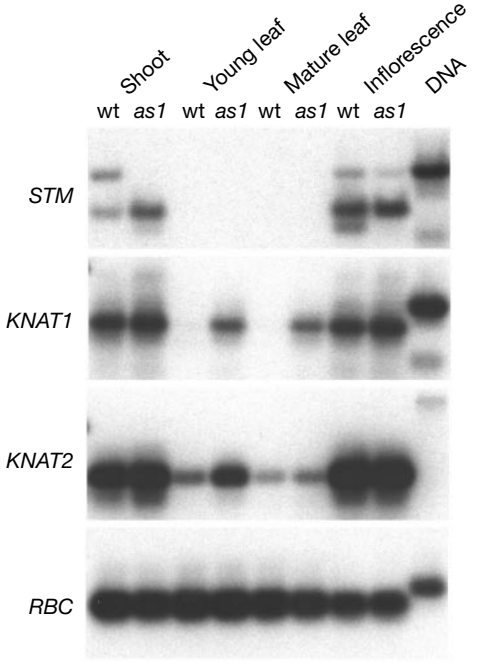

Figure 2 Polymerase chain reaction after reverse transcription of RNA (RT–PCR) analysis of *KNOX* gene expression in *as1* and wild type. RNA was extracted from shoots, young leaves, mature leaves and inflorescence tissues. RT–PCR reactions were performed using gene-specific primers. Products were blotted and hybridized with gene-specific probes. *STM* is detected in wild type (wt) and *as1* shoot and inflorescence, and not in leaf tissue. *KNAT1* is detected in wild type and *as1* shoot and inflorescence and is found in *as1* leaf tissue. *KNAT2* is detected in all tissues in wild type and *as1* but is upregulated in young leaves and, to a lesser extent, in mature leaves of *as1*. *RBC* transcripts were amplified as a control.

AS1 in a gene closely related to the myb transcription factor *PHAN*, which had previously been named *Atphan*[11]. Two independent *as1* alleles were sequenced and found to have mutations in *Atphan* predicted to truncate the carboxy-terminal third of the AS1 protein. *as1-magnifica* was found to result from a rearrangement at the 5′ end of the gene (likely inversion) that disrupts the promoter. A 6-kilobase (kb) genomic fragment encompassing *Atphan* complemented *as1-1* (see Methods). Together, these results confirmed that *Atphan* is *AS1*.

The expression pattern of *AS1* was examined by *in situ* hybridization. In wild-type embryos *AS1* RNA first became detectable in late globular stage, predominantly in two subepidermal domains corresponding to cotyledon initials (Fig. 3a). Expression was maintained in subepidermal cells of developing cotyledons from heart stage onwards, but was absent or reduced in cells that would subsequently form the shoot apical meristem and the cotyledon epidermis (Fig. 3b–e). After germination, *AS1* was detected in leaf founder cells from the time of primordium initiation until stage P4 and in cells associated with the cotyledon vasculature (Fig. 3f). On flowering, *AS1* RNA was detected on the flank of the inflorescence apex in a region corresponding to the "cryptic bract" (Fig. 3g)[21]. In early floral primordia *AS1* expression was first detected in the abaxial sepal primordium (Fig. 3g), and subsequently in primordia of all floral organs (Fig. 3h). This is consistent with reduced growth of these organs in *as1* flowers[15].

Our analysis of *KNOX* gene expression in *as1* showed misexpression of *KNAT1* and *KNAT2*, whereas *STM* expression was unchanged. To place *STM* in a genetic pathway relative to *AS1*, double mutants were made using a strong allele of *stm*. Embryos homozygous for *stm-1* lack a SAM and develop cotyledons that are fused at their base (Fig. 4b)[4,5]. F2 progeny from a cross between *stm-1*/+ × *as1-1*/*as1-1* segregated, at a ratio of 1/16, a novel phenotype identified as the *as1-1 stm-1* double mutant (see Methods). Double-mutant vegetative shoots and leaves were indistinguishable from *as1* single mutants (Fig. 4a and c), indicating that the embryonic and vegetative phenotype of *stm-1* was completely suppressed by loss of *AS1* activity. Epistasis of *as1* also demonstrated that the *as1* mutant phenotype was not dependent on *STM* activity, consistent with RT–PCR data showing that these plants do not misexpress *STM*.

In reproductive development, *as1-1 stm-1* double mutants differed from *as1* single mutants in continuing to generate lateral shoots, each subtended by a cauline leaf, instead of flowers (Fig. 4c). The overall shoot architecture was comparable to wild-type plants, although occasional flowers that formed resembled those conditioned by weak alleles of *stm* (Fig. 4d)[5,22]. The double-mutant phenotype showed that loss of *AS1* activity in *as1-1* was insufficient to suppress the *stm* mutant phenotype in reproductive development.

Genetic interaction between *as1* and *stm* demonstrates that *as1* can rescue the *stm* phenotype in embryonic and vegetative meristems. Given that the two genes are expressed in complementary domains, and that the expression pattern of *STM* does not change in *as1* mutants, we conclude that *STM* negatively regulates *AS1*. *In situ* hybridization of siliques (fruits) segregating 1/4 *stm* embryos revealed *AS1* expression throughout the apical half of 13 out of 60 heart stage embryos consistent with this conclusion (Fig. 3l–k).

The genetic and molecular interaction between *AS1* and *KNOX* genes allows us to propose a mechanism by which organ founder cells are distinguished from stem cells and their derivatives in the shoot apical meristem. In stem cells *STM* negatively regulates *AS1*.

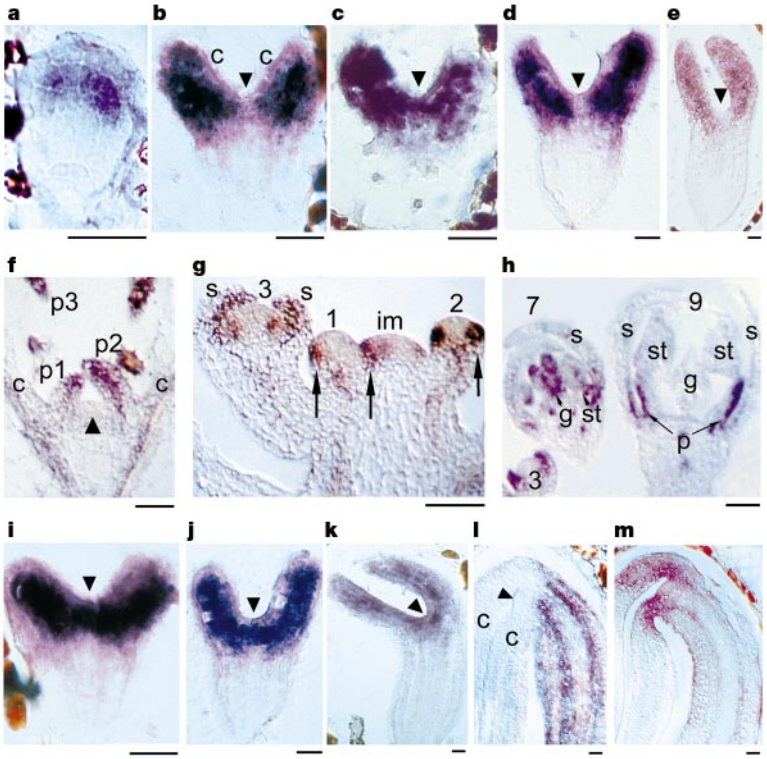

Figure 3 Expression of *AS1* and *KNAT1*. *In situ* hybridization showing expression of *AS1* (**a**–**k**) and *KNAT1* (**l**, **m**) in wild-type embryos at successive stages of development (**a**–**e**), wild-type vegetative apex (**f**) and inflorescence apices (**g**, **h**), *stm-1* mutant (**i**–**k**), wild type (**l**) and *as1* (**m**) embryos. **b** and **c** are two sections from the same embryo taken 7 μm apart. Arrowheads indicate SAM cells or their initials. Arrows in **g** indicate cryptic bract and initials of the lowermost sepal. *AS1* expression is confined to organ primordia and is absent from the SAM. In *as1* mutants *KNAT1* is ectopically expressed at the base of the cotyledons. c, cotyledon, im, inflorescence meristem, s, sepal, p, petal, st, stamen, g, gynoecium, p1–p3, leaves of increasing developmental age. Scale bars, 25 μm.

In founder cells, *STM* is downregulated, allowing *AS1* to be expressed. *AS1* in turn downregulates *KNAT1* and *KNAT2*. Thus, *stm* mutant embryos fail to develop a meristem owing to misexpression of *AS1* in presumptive stem cells and their immediate derivatives, causing them to lose their undifferentiated meristematic state. In the *as1 stm-1* double mutant, lack of *AS1* allows meristem function in the absence of *STM*, potentially promoted by derepression of *KNAT1* and *KNAT2*. These *KNOX* genes are closely related to *STM*[7], although their ability to complement the *stm* phenotype is not known. In floral promordia *STM* has a function independent of *AS1*. The network of negative gene interactions between *AS1* and *KNOX* genes functions to distinguish between stem cells and founder cells within the SAM. This leads to a situation in which *STM* is not required for SAM formation in the absence of *AS1*. In contrast, several other genes known to interact with *STM*, including the *CLV* genes, *WUS* and *CUC2* (refs 23, 24, 25), are all expressed in regions of the SAM and are required for meristem function. Mutations in *CLV1*, *CLV3* and *WUS* show additive interactions with *as1*, demonstrating that *AS1* acts independently of these genes (not shown). This is consistent with *AS1* and *STM* acting in a parallel pathway to *WUS* and *CLV* to specify cell fate in the meristem[5,22].

AS1, *PHAN* and *RS2* all negatively regulate *KNOX* gene expression in organ primordia, demonstrating a degree of functional conservation in *Arabidopsis*, *Antirrhinum* and maize. In maize, *rs2* mutants show alterations along the leaf proximodistal axis, with proximal sheath and ligule tissues displaced distally into the leaf blade[14]. *as1* mutants show changes in the proximodistal and mediolateral axes, resulting in characteristic leaf asymmetry (Fig. 1). In *Antirrhinum*, lower leaves of *phan* mutants are broad and heart-shaped with prominent veins similar to those of *as1*. *phan* in addition affects the dorsoventral and proximodistal axes in a cold-sensitive fashion[10,12]. Upper *phan* leaves are radial and ventralized, and fail to grow out altogether at restrictive temperatures. In contrast, *as1* and *rs2* do not form radialized leaves. *Arabidopsis* and *Antirrhinum* are both eudicots with simple leaves, and fundamental aspects of leaf development are expected to be similar in the two species. The differences between *as1* and *phan* phenotypes may reflect allelic differences or functional divergence of these genes and their targets. Alternatively, they might be explained by modifiers in *Antirrhinum* that enhance *phan* in upper leaves. □

Figure 4 *as1* shows genetic interaction with *stm-1*. **a**, *as1* whole-plant phenotype. Rosette and cauline leaves are rounded and lobed. After 3–5 cauline leaves with associated secondary shoots, flowers form on the main inflorescence and lateral shoots. **b**, *stm-1* mutants showing cotyledons fused at the base and no vegetative shoot. **c**, *as1 stm-1* double mutant. Rosette is indistinguishable from *as1* single mutants. The main inflorescence and lateral shoots fail to produce flowers, but continue to form lateral shoots with subtending cauline leaves. **d**, *as1 stm-1* double mutant flower. Occasional flowers formed on double mutants typically have reduced petal and stamen number and no central carpel. Floral organs are sometimes mosaic (arrow).

Methods

Plant stocks and growth conditions

All alleles of *as1* (*magnifica*, *as1-1* and *as1-17*) and *stm* used in this study were obtained from the Arabidopsis Biological Resource Center (ARBC). Gene and enhancer trap lines were generated as previously described[26]. Plants were grown either on soil or on Murashige and Skoog salts media[26], supplemented with vitamins, with a minimum day length of 16 h. GUS staining was carried out as previously described[26].

Genetic analysis

as1 was mapped relative to *det2* by progeny testing the F2 plants from the cross *cp er as1 cer8* × *det2*. Out of 100 recombinants between *as1* and *cer8*, three carried the haplotype *cp er as1 det2*, placing *as1* 0.3 cM proximal to *det2*. A second cross between *hy1 as1* and ecotype Landsberg *erecta* identified recombinants proximal to *as1*. Molecular mapping of recombinants between *hy1* and *as1* was carried out using derived (this study) and previously identified CAPS markers (ARBC)[27]. To construct double mutants, plants homozygous for *as1-1* were crossed as males to plants heterozygous for *stm-1*. Double *as1-1 stm1* mutants segregated in the F2 progeny in the expected 1:15 ratio; percentage segregation for each phenotypic class were wild-type (55.8%): *as1* (17.4%): *stm-1* (21.2%): *as1 stm-1* (5.6%). The *stm-1* genotype of double mutants was confirmed by a PCR assay. For each DNA template a common primer GCCCATCATGACATCACATC was used in separate reactions with a primer, CTTTAAGCTCTCTATCCTCAGCTTG, designed to amplify the wild-type STM allele and a primer, CTTTAAGCTCTCTATCCTC AGCTTA, designed to amplify the mutant *stm-1* allele[17]. Standard PCR reaction conditions were used with an annealing temperature of 66 °C.

DNA and RNA analysis

DNA extraction and manipulation were as described previously[28]. Total RNA was purified using Trizol reagent (GibcoBRL). Following DNase treatment (Boehringer Mannheim) complementary DNA was synthesized using M-MuLV reverse transcriptase (New England Biolab) in 50 mM Tris-HCl (pH 8.3), 30 mM KCl, 8 mM $MgCl_2$, 10 mM DTT, 1 mM each of dATP, dCTP, dGTP, dTTP, 1 μM oligo dT, 50 units RNasin, 0.1 μg BSA and 100 units reverse transcriptase. RT–PCR reactions were performed with gene specific primers and products were subject to Southern hybridization using specific probes amplified or subcloned from each gene.

Cloning and sequencing

For complementation a 6-kb genomic fragment encompassing the *AS1* (At2g37630) locus was cloned into the vector pPZP112 (ref. 29) and transformed by *Agrobacterium* into plants. To sequence *as1-1* and *as1-17* alleles genomic DNA from homozygous plants was amplified with the primers ACATTGGAGACACCCAAATGA and CCCTGTTTGGTTT-CCAGAATA, encompassing the coding region of *AS1*. PCR products were sequenced with internal primers, using the dye terminator cycle sequencing (Applied Biosystems). TAIL-PCR[30] was used to determine the sequence disruption in the *magnifica* allele.

Scanning electron microscopy

Fresh material was mounted on silver tape (Electron Microscope Sciences) and viewed with an Hitachi S-3500N SEM using a beam voltage of 5 kV.

In situ hybridization

AS1 RNA was detected with a digoxigenin-labelled riboprobe complementary to part of the *AS1* transcript downstream of the conserved *MYB* domain (C-terminal 124 amino acids) using the method of ref. 21 (http://www.wisc.edu/genetics/CATG/ barton/protocols.html).

Received 4 June; accepted 23 October 2000.

1. Martienssen, R. & Dolan, L. in *Arabidopsis. Annual Plant Reviews* (eds Anderson, M. & Roberts, J.) 262–297 (Sheffield Academic Press, Sheffield, 1998).

2. Hudson, A. Development of symmetry in plants. *Annu. Rev. Plant. Physiol. Mol. Biol.* **51,** 349–370 (2000).
3. Jackson, D., Veit, B. & Hake, S. Expression of maize *KNOTTED1* related homeobox genes in the shoot apical meristem predicts patterns of morphogenesis in the vegetative shoot. *Development* **120,** 405–413 (1994).
4. Barton, M. K. & Poethig, R. S. Formation of the shoot apical meristem in *Arabidopsis thaliana*—an analysis of development in the wild type and in the *shoot meristemless* mutant. *Development* **119,** 823–831 (1993).
5. Clark, S. E., Jacobsen, S. E., Levin, J. Z. & Meyerowitz, E. M. The *CLAVATA* and *SHOOT MERISTEMLESS* loci competitively regulate meristem activity in *Arabidopsis*. *Development* **122,** 1567–1575 (1996).
6. Vollbrecht, E., Reiser, L. & Hake, S. Shoot meristem size is dependent on inbred background and presence of the maize homeobox gene, *knotted1*. *Development* **127,** 3161–3172 (2000).
7. Reiser, L., Sanchez-Baracaldo, P. & Hake, S. Knots in the family tree: evolutionary relationships and functions of *knox* homeobox genes. *Plant Mol. Biol.* **42,** 151–166 (2000).
8. Sinha, N. R., Williams, R. E. & Hake, S. Overexpression of the maize homeo box gene, *KNOTTED-1*, causes a switch from determinate to indeterminate cell fates. *Genes Dev.* **7,** 787–795 (1993).
9. Chuck, G., Lincoln, C. & Hake, S. *Knat1* induces lobed leaves with ectopic meristems when overexpressed in *Arabidopsis*. *Plant Cell* **8,** 1277–1289 (1996).
10. Waites, R., Selvadurai, H. R., Oliver, I. R. & Hudson, A. The *PHANTASTICA* gene encodes a MYB transcription factor involved in growth and dorsoventrality of lateral organs in *Antirrhinum*. *Cell* **93,** 779–789 (1998).
11. Timmermans, M. C., Hudson, A., Becraft, P. W. & Nelson, T. ROUGH SHEATH2: a Myb protein that represses *knox* homeobox genes in maize lateral organ primordia. *Science* **284,** 151–153 (1999).
12. Waites, R. & Hudson, A. *phantastica*: a gene required for dorsoventrality of leaves in *Antirrhinum majus*. *Development* **121,** 2143–2154 (1995).
13. Tsiantis, M., Schneeberger, R., Golz, J. F., Freeling, M. & Langdale, J. A. The maize *rough sheath2* gene and leaf development programs in monocot and dicot plants. *Science* **284,** 154–156 (1999).
14. Schneeberger, R., Tsiantis, M., Freeling, M. & Langdale, J. A. The *rough sheath2* gene negatively regulates homeobox gene expression during maize leaf development. *Development* **125,** 2857–2865 (1998).
15. Reidei, G. P. Non-mendelian megagametogenesis in *Arabidopsis*. *Genetics* **51,** 857–872 (1965).
16. Reinholz, E. *Arabidopsis thaliana* (L.) HEYNH. als Objekt fur genetische und entwicklungsphysiologische Untersuchungen. *Arabidopsis Inform. Service* **01S,** 24 (1965).
17. Long, J. A., Moan, E. I., Medford, J. I. & Barton, M. K. A member of the KNOTTED class of homeodomain proteins encoded by the *STM* gene of *Arabidopsis*. *Nature* **379,** 66–69 (1996).
18. Lincoln, C., Long, J., Yamaguchi, J., Serikawa, K. & Hake, S. A *knotted1*-like homeobox gene in *Arabidopsis* is expressed in the vegetative meristem and dramatically alters leaf morphology when overexpressed in transgenic plants. *Plant Cell* **6,** 1859–1876 (1994).
19. Dockx, J. *et al.* The homeobox gene *ATK1* of *Arabidopsis thaliana* is expressed in the shoot apex of the seedling and in flowers and inflorescence stems of mature plants. *Plant Mol. Biol.* **28,** 723–737 (1995).
20. Lin, X. *et al.* Sequence and analysis of chromosome 2 of the plant *Arabidopsis thaliana*. *Nature* **402,** 761–768 (1999).
21. Long, J. & Barton, M. K. Initiation of axillary and floral meristems in *Arabidopsis*. *Dev. Biol.* **218,** 341–353 (2000).
22. Endrizzi, K., Moussian, B., Haecker, A., Levin, J. Z. & Laux, T. The *SHOOT MERISTEMLESS* gene is required for maintenance of undifferentiated cells in *Arabidopsis* shoot and floral meristems and acts at a different regulatory level than the meristem genes *WUSCHEL* and *ZWILLE*. *Plant J.* **10,** 101–113 (1996).
23. Clark, S. E., Running, M. P. & Meyerowitz, E. M. *CLAVATA3* is a specific regulator of shoot and floral meristem development affecting the same processes as *CLAVATA1*. *Development* **121,** 2057–2067 (1995).
24. Mayer, K. F. *et al.* Role of *WUSCHEL* in regulating stem cell fate in the *Arabidopsis* shoot meristem. *Cell* **95,** 805–815 (1998).
25. Aida, M., Ishida, T. & Tasaka, M. Shoot apical meristem and cotyledon formation during *Arabidopsis* embryogenesis: interaction among the *CUP-SHAPED COTYLEDON* and *SHOOT MERISTEMLESS* genes. *Development* **126,** 1563–1570 (1999).
26. Sundaresan, V. *et al.* Patterns of gene action in plant development revealed by enhancer trap and gene trap transposable elements. *Gene Dev.* **9,** 1797–1810 (1995).
27. Li, J., Nagpal, P., Vitart, V., McMorris, T. C. & Chory, J. A role for brassinosteroids in light-dependent development of *Arabidopsis*. *Science* **272,** 398–401 (1996).
28. Springer, P. S., McCombie, W. R., Sundaresan, V. & Martienssen, R. A. Gene trap tagging of *PROLIFERA*, an essential *MCM2-3-5*-like gene in *Arabidopsis*. *Science* **268,** 877–880 (1995).
29. Hajdukiewicz, P., Svab, Z. & Maliga, P. The small, versatile pPZP family of *Agrobacterium* binary vectors for plant transformation. *Plant Mol. Biol.* **25,** 989–994 (1994).
30. Liu, Y. G., Mitsukawa, N., Oosumi, T. & Whittier, R. F. Efficient isolation and mapping of *Arabidopsis thaliana* T-DNA insert junctions by thermal asymmetric interlaced PCR. *Plant J.* **8,** 457–463 (1995).

Acknowledgements

We thank A. Groover, C. Kidner, E. Vollbrecht, M. Timmermans, J. Golz and D. Jackson for helpful discussions, Q. Gu, P. Springer, J. Li and J. Chory for help with mapping and T. Laux for wus-1 seed. We also thank T. Mulligan for plant care, and K. Schutz and D. McCombie for help with sequencing. This work was supported by a Human Frontiers Science Program postdoctoral fellowship to M.C., a Biotechnology and Biological Sciences Research Council studentship to R.B. and grant support from the National Science Foundation, Department of Energy and United States Department of Agriculture to R.M.

Correspondence and requests for materials should be addressed to R.M. (e-mail: martiens@cshl.org).

Neuronal switching of sensorimotor transformations for antisaccades

Mingsha Zhang & Shabtai Barash

Department of Neurobiology, Weizmann Institute of Science, Rehovot, Israel

The influence of cognitive context on orienting behaviour can be explored using the mixed memory-prosaccade, memory-antisaccade task. A symbolic cue, such as the colour of a visual stimulus, instructs the subject to make a brief, rapid eye movement (a saccade) either towards the stimulus (prosaccade) or in the opposite direction (antisaccade)[1–3]. Thus, the appropriate sensorimotor transformation must be switched on to execute the instructed task. Despite advances in our understanding of the neuronal processing of antisaccades[4–8], it remains unclear how the brain selects and computes the sensorimotor transformation leading to an antisaccade. Here we show that area LIP of the posterior parietal cortex is involved in these processes. LIP's population activity turns from the visual direction to the motor direction during memory-antisaccade trials. About one-third of the visual neurons in LIP produce a brisk, transient discharge in certain memory-antisaccade trials. We call this discharge 'paradoxical' because its timing is visual-like but its direction is motor. The paradoxical discharge shows, first, that switching occurs already at the level of visual cells, as previously proposed by Schlag-Rey and colleagues[5]; and second, that this switching is accomplished very rapidly, within 50 ms from the arrival of the visual signals in LIP.

Figure 1a illustrates the problem raised in ref. 5. At the core of the sensorimotor transformation guiding antisaccades lies vector inversion. How does the brain compute this inversion? Figure 1b sketches relevant processing at the single-cell level. Figure 1b refers to visual and motor activity; a standard criterion for distinguishing between visual and motor activity is by timing the activity in memory-saccades[9–15], as shown below. For brevity, we call cells with visual activity 'visual cells', and cells with motor activity 'motor cells'. Although Fig. 1b is simplistic, it provides a framework for the two hypotheses we will consider for task switching. Both hypotheses propose that prosaccades and antisaccades involve alternative sets of functional connections between cells. A standard set of connections leads to prosaccades. A different set of connections, that emerges during training, leads to antisaccades. An instruction to perform an antisaccade switches the set of active connections from one configuration to the other.

According to the "visual switching hypothesis" (proposed in ref. 5), the switched connections are between visual cells. The process of switching connections would be reflected in a critical set of visual cells, each having two alternative receptive fields, a standard receptive field for ordinary prosaccades and another receptive field in the opposite direction specifically for antisaccades. Activation of the new receptive field, through the new connections, would instigate vector inversion. Thus, vector inversion would be accomplished by receptive field remapping[16]. The "visuomotor switching hypothesis" proposes that switching acts on connections between visual and motor cells. The two hypotheses lead to contrasting experimental predictions with regard to each cell's visual receptive field (mapped relative to the visual vector) and motor field (mapped relative to the motor vector) in prosaccades and antisaccades. The visuomotor switching hypothesis predicts that both visual and motor fields remain unchanged, in all cells. Although a critical set of cells with motor activity would fire in trials with opposite visual vectors in prosaccades and antisaccades, the motor fields of these cells would not change. In contrast, the visual switching hypothesis predicts changed receptive fields for some